MIT Libraries | DSpace@MIT

MIT Open Access Articles

Quantum Rate Coefficients and Kinetic Isotope Effect for the Reaction Cl + CH[subscript 4] → HCl + CH[subscript 3] from Ring Polymer Molecular Dynamics

The MIT Faculty has made this article openly available. ***Please share*** how this access benefits you. Your story matters.

Citation: Li, Yongle, Yury V. Suleimanov, William H. Green, and Hua Guo. "Quantum Rate Coefficients and Kinetic Isotope Effect for the Reaction Cl + CH[subscript 4] → HCl + CH[subscript 3] from Ring Polymer Molecular Dynamics." The Journal of Physical Chemistry A 118, no. 11 (March 20, 2014): 1989–1996.

As Published: http://dx.doi.org/10.1021/jp501043z

Publisher: American Chemical Society (ACS)

Persistent URL: http://hdl.handle.net/1721.1/95491

Version: Author's final manuscript: final author's manuscript post peer review, without publisher's formatting or copy editing

Terms of Use: Article is made available in accordance with the publisher's policy and may be subject to US copyright law. Please refer to the publisher's site for terms of use.

Massachusetts Institute of Technology

Submitted to J. Phys. Chem. A. 12/2/2013, revised 1/23/2014

Quantum rate coefficients and kinetic isotope effect for the reaction Cl + CH_4 → HCl + CH_3 from ring polymer molecular dynamics

Yongle Li,[1] Yury V. Suleimanov,[2,3,] William H. Green,[2] and Hua Guo[1,*]*

[1]*Department of Chemistry and Chemical Biology, University of New Mexico, Albuquerque, NM 87131, USA*

[2]*Department of Chemical Engineering, Massachusetts Institute of Technology, Cambridge, MA 02139, USA*

[3]*Department of Mechanical and Aerospace Engineering, Combustion Energy Frontier Research Center, Princeton University, Olden St., Princeton, New Jersey 08544, USA*

* corresponding authors: ysuleyma@mit.edu, hguo@unm.edu

Abstract

Thermal rate coefficients and kinetic isotope effects have been calculated for prototypical heavy-light-heavy polyatomic bimolecular reactions Cl + CH_4/CD_4 → HCl/DCl + CH_3/CD_3, using a recently proposed quantum dynamics approach - ring polymer molecular dynamics (RPMD). Agreement with experimental rate coefficients, which are quite scattered, is satisfactory. However, unexpected differences have been found between the RPMD results and those obtained from variational transition-state theory for two full-dimensional potential energy surfaces used in the calculations. Possible reasons for such discrepancy are discussed. The present work is an important step in a series of benchmark studies aimed at assessing accuracy for RPMD for chemical reaction rates which demonstrates that this novel method is a quite reliable alternative to previously developed techniques based on transition-state theory.

I. Introduction

The reaction between chlorine atom and methane is of great importance in atmospheric chemistry.[1,2,3] Many kinetic measurements have been reported[4-15] and the rate coefficients near room temperature have been critically evaluated.[16-17] A particularly interesting issue is the fractionation of methane isotopomers in the atmosphere, which yields unique isotopic signatures.[18-19] These kinetic isotope effects (KIEs) stems from isotopic-dependent reaction rates, which are quite significant for the title reaction due to its tunneling nature, particularly at low temperatures.

This reaction is one of prototypical polyatomic bimolecular reactions.[20-23] This heavy-light-heavy reaction presents a challenge to transition-state theory[24-28] because of the strong tunneling and recrossing dynamics.[29] In addition, it has served as a testing ground for mode and bond selectivity in bimolecular reactions.[30-34] As the reaction involves the transfer of a hydrogen atom, its dynamics and kinetics need be treated quantum mechanically to accurately describe quantum effects, such as tunneling and zero-point energy. However, an accurate full-dimensional quantum characterization of the reaction dynamics remains a formidable challenge because it requires twelve coordinates.[35] So far, all quantum dynamical calculations on this reaction have been based on reduced-dimensional models.[36-41] Fortunately, the accurate determination of the rate coefficients does not necessarily need all the state-to-state attributes because the reactivity is essentially controlled by the transition state.[42] In this work, we compute the canonical rate coefficients for the title reactions using the recently proposed ring polymer molecular dynamics (RPMD) method,[43] which can be considered as an approximate quantum mechanical approach with full dimensionality. RPMD differs from the

traditional transition-state theory methods, which are based on various static approximations to the real-time correlation functions used to describe chemical reactions, in its explicit, though approximate, consideration of the real-time dynamics.[43] This feature can be particularly important for systems similar to the title reaction, which is affected not only by tunneling, but also by strong recrossing of the transition state due to the chattering motion of the transferring hydrogen between two heavy atoms. Hence, the present work can be considered as an important step in a series of benchmark studies aimed at assessing accuracy of RPMD for various complex polyatomic systems. This publication is organized as follows. The RPMD theory and computational details are outlined in Sec. II. The results are presented and discussed in Sec. III, and conclusions are given in Sec. IV.

II. Theory

The ring polymer molecular dynamics (RPMD) method[43] exploits the isomorphism between the statistical properties of a quantum system and those of a fictitious classical ring polymer made up of harmonically connected beads.[44] Its adaptation to the calculation of rate coefficients for chemical reactions has been shown to have several desirable features.[45-47] For example, the RPMD rate coefficient approaches the classical limit at high temperatures. It also has a well-defined short-time limit that serves as an upper bound of the RPMD rate. More recently, it was shown that it is equivalent to the quantum transition-state theory in the limit of no recrossing.[48,49] Furthermore, the RPMD rate coefficient is independent of the choice of the dividing surface, which is highly desirable because the dividing surface is difficult to define for high-dimensional systems. RPMD is accurate even in the deep tunneling regime due to a

connection to semi-classical instanton theory.[49] Finally, it is numerically efficient because of the favorable scaling laws associated with classical trajectories. The RPMD approach has been successfully employed to obtain accurate rate coefficients for several bimolecular reactions, in which comparison with full-dimensional quantum dynamical calculations indicated that RPMD reliably captures quantum effects such as zero-point energy and tunneling.[50-58]

Taking advantage of the Bennett-Chandler factorization,[59-60] the RPMD rate can be conveniently presented in the following form:[50-51, 61]

$$k_{\mathrm{RPMD}} = k_{\mathrm{QTST}}(T;\xi^{\neq})\kappa(t\to\infty;\xi^{\neq}). \tag{1}$$

The first term denotes the static contribution while the second is the dynamical correction. In particular, $k_{\mathrm{QTST}}(T;\xi^{\neq})$ is the centroid-density quantum transition-state theory (QTST) rate coefficient,[47, 62] evaluated at the top of the free energy barrier, $\xi^{\neq}$, along the reaction coordinate $\xi(\boldsymbol{q})$. This quantity depends on the position of the dividing surface and is determined entirely by static equilibrium properties. In practice, it is calculated from the centroid potential of mean force (PMF):[50-51, 61]

$$k_{\mathrm{QTST}}(T,\xi^{\neq}) = 4\pi R_{\infty}^{2}\left(\frac{1}{2\pi\beta\mu_{\mathrm{R}}}\right)^{1/2} e^{-\beta\left[W(\xi^{\neq})-W(0)\right]}, \tag{2}$$

where μ_{R} is the reduced mass between the two reactants, $\beta=(k_B T)^{-1}$ and $W(\xi^{\neq})-W(0)$ is the free-energy difference which is obtained via umbrella integration along the reaction coordinate.[61, 63-64]

The dynamical correction is provided by the second factor ($\kappa(t \to \infty; \xi^{\neq})$) in Eq. (1), which is the long-time limit of a time-dependent ring-polymer transmission coefficient accounting for recrossings at the top of the free-energy barrier ($\xi^{\neq}$). This factor counterbalances $k_{\mathrm{QTST}}(T; \xi^{\neq})$, ensuring the independence of the RPMD rate coefficient $k_{\mathrm{RPMD}}(T)$ of the choice of the dividing surface.[47, 64]

An added advantage of the RPMD rate theory is that it approaches the classical limit when only one bead is used. In this limit, the static and dynamical components of Eq. (1) become identical to the classical transition-state theory rate coefficient and the classical transmission coefficient, respectively.[50] These quantities thus establish the limit to which the quantum effects such as ZPE and tunneling can be evaluated by using more beads. The minimal number of beads needed to account for the quantum effects can be estimated by the following formula:[53]

$$n_{\min} \equiv \beta \mathrm{h} \omega_{\max}, \tag{3}$$

where $\omega_{\max}$ is the largest vibrational frequency of the system.

All calculations reported here used RPMDrate developed by Suleimanov and co-workers and the remaining details of the computational procedure can be found in the RPMDrate manual.[61] The calculations are first performed with one bead, which provides the classical limit. The number of beads was then increases until convergence. Two full-dimensional analytical PESs were used in our RPMD calculations in the range of 300-1000 K. The first was an empirical PES calibrated to limited *ab initio* data by Espinosa-Garcia and coworkers (RNCE).[65] This PES was chosen because it has been used for

many previous theoretical studies,[65] including a rate coefficient calculation using the canonical unified statistical model with the microcanonical optimized multidimensional tunneling correction (CUS/μOMT).[24] The other is the more recent PES developed by Czako and Bowman (CB) based on a large number of high-level ab initio points.[66] The evaluation of the latter is much slower. As a result, we have computed the rate coefficients only at only two temperatures (600 and 1000 K) for the $Cl + CH_4$ reaction.

In the calculation of the PMF, windows with an equal size ($\Delta\xi$=0.01) is used and the force constant of the biasing potential is k=2.72 (T/K) eV. In each sampling window, the system was first equilibrated for 20 ps, following by a production run (20 ns and 5 ns on RNCE PES and CB PES, respectively). The Andersen thermostat[67] is used in all simulations. The time step is 0.1 and 0.5 fs on RNCE and CB PESs, respectively. Due to the larger time step and shorter simulation time, the results on the CB PES are expected to be less accurate. However, tests on the RNCE PES using the same parameters indicated that the error is within 5% that we expect for the total calculation.

After the PMF calculations, the transmission coefficients are computed. This was initiated by running a long (20 ns) mother trajectory with the ring-polymer centroid fixed at the top of the free energy barrier via the SHAKE algorithm.[68] Configurations are sampled once every 2 ps to serve as the initial positions for the child trajectories used to compute the flux-side correlation functions. For each initial position, 100 separate ring polymer trajectories are spawned with different initial momenta sampled from the Boltzmann distribution. These trajectories were then propagated with no constraint for 0.1 ps where the transmission coefficients reach plateau values. The time step in this stage is set to 0.1 fs for both PESs.

The final RPMD rate coefficients are corrected with an electronic partition function ratio of the following form:

$$\frac{Q_{\mathrm{elec}}^{\mathrm{TS}}}{Q_{\mathrm{elec}}^{\mathrm{reactants}}} = \frac{1}{2+\exp(-\beta\Delta E)}, \tag{4}$$

in order to take into account the spin-orbit splitting of $Cl(^2P_{1/2,3/2})$ (ΔE=882 cm^{-1})atom.[70]

III. Results and discussion

The RPMD rate coefficients for the Cl + CH_4 reaction obtained on the RNCE and CB PESs are listed in Table 1 and those for the Cl + CD_4 reaction are given in Table 2. It is clear from these tables that the hydrogen/deuterium abstraction reactions are characterized by strong recrossing, as evidenced by much smaller RPMD transmission coefficients than those in the H/O + CH_4 reactions.[53, 55] Recrossing, which is a well-known feature of heavy-light-heavy reactions,[29] is used here loosely as it not only include classical recrossing over the barrier, but also quantum mechanical tunneling. Indeed, the RPMD transmission coefficients are larger for the Cl + CD_4 reaction, reflecting the less facile transfer of the heavier deuterium atom. In both cases, the transmission coefficients generally increase with temperature, as seen in the previous RPMD studies.[50-51, 55-56]

In Fig. 1, the time-dependence of the computed transmission coefficients is shown for both Cl + CH_4 and Cl + CD_4 reactions on the RNCE PES. It is clear that they experience a fast initial drop apparently due to recrossing near the barrier. This is followed by some oscillations, particularly at low temperatures. Such oscillatory behavior has been observed in the previous RPMD studies.[52, 54-55, 64] The time required for converging the correlation functions for these two reactions (~0.1 ps at 300 K) is

significantly longer than that required for the H + CH_4 reaction,[55] in which the transmission coefficients take only 30 fs to reach the plateau value, consistent with the relatively long-lived recrossing dynamics.

The RPMD rate coefficients for the Cl + CH_4 reaction are compared in Fig. 2a with the previous CUS/μOMT results on the RNCE PES.[65] In addition, the rate coefficients obtained with the CVT/μOMT (CVT for canonical variational transition-state theory) method are also included in comparison. These TST results were generated using POLYRATE using curvilinear coordinates and the harmonic approximation for the vibrational partition functions,[69] and the CUS/μOMT results of Rangel *et al*.[65] on the RNCE PES were reproduced. Interestingly, the CUS/μOMT and CVT/μOMT results are very close at high temperatures (10% deviation at 1000 K). The RPMD rate coefficients are somewhat larger than the CUS/μOMT and CVT/μOMT counterparts, except at low temperatures. The difference increases with increasing the temperature. This result is unusual because initially we expected to see the RPMD rate coefficient to be smaller than the TST counterparts at high temperatures. This is because RPMD is exact in the high-temperature limit and TST calculations for heavy-light-heavy systems could overestimate the rate due to ignoring recrossing. Also, we expected the role of recrossing to decrease with increasing temperature getting RPMD and TST calculations closer to each other and to the classical TST.

Several considerations should be taken into account when trying to find possible explanations for this discrepancy. First, RPMD is known to overestimate the rate constant for asymmetric reactions.[50] However, this is expected to happen at low temperatures in

the so-called deep-tunneling regime.[50] At high temperatures, such as 1000 K, tunneling should play less important role than ZPE effect for current system because the crossover temperature is 178 K. At high temperatures, RPMD is expected to be very reliable and close to the exact quantum mechanical result and to converge to it in the high-temperature limit (where quantum and classical results coincide).[50-51] Second, the quantum mechanical interference effects in the real time dynamics such as quantum reactive scattering resonances tend to be more pronounced for reactions with a small skew angle, such as the Cl + CH_4 reaction. However, these effects are not included in any of the computations shown here and, in the absence of the exact QM results, it is difficult to elucidate their role in the thermal rate coefficients. Third, the TST results might underestimate the rate coefficient at high temperatures due to the harmonic approximation employed. We have carried out a purely classical calculation at 1000 K by using RPMDrate code and RNCE PES with the same calculation parameters but with one ring polymer bead,[51] which ignores all quantum effects. The classical rate coefficient corrected for the recrossing dynamics calculated by using RPMDrate is 5.52×10^{-12} s^{-1} $molecule^{-1}$ cm^3, which is about half of the RPMD rate coefficient (1.23×10^{-11} s^{-1} $molecule^{-1}$ cm^3). The difference between these two calculations shows that quantum effects are important for this reaction and their improper treatment could lead to a noticeable error in the rate coefficient even at 1000 K. Another reason could be semi-empirical nature of the RNCE PES and its possible inaccuracy for full dynamics calculations such as RPMD. Indeed, questions concerning this type of PES have been raised by Varandas and coworkers some time ago.[72] However, we note all these considerations do not explain the unusually large discrepancy between RPMD and TST

calculations and further investigations are required in order to elucidate the real reason for it. We suggest that rigorous quantum mechanical calculations, which should become possible in the near future, will be of invaluable help in solving this puzzle.

In Fig. 2b, the RPMD rate coefficients obtained on the *ab initio* based CB PES are compared with results obtained by the two versions of TST. It is interesting to note that although the CUS/μOMT and CVT/μOMT results are quite similar on the RNCE PES, the difference is much larger on the CB PES. More importantly, the RPMD values are very close to CUS/μOMT ones, but are smaller than the CVT/μOMT counterparts. This behavior is in line with our initial expectations, further suggesting that the puzzling results we obtained for RNCE PES might be due to some special feature of the RNCE PES. However, we note again that only rigorous quantum mechanical calculations can confirm or refute our speculations.

In Fig. 2c, the RPMD rate coefficients on both PESs are compared with representative experimental results. RPMD rate coefficients obtained on the *ab initio* based CB PES are somewhat lower those on the RNCE PES, reflecting the higher free-energy barrier in the *ab initio* PES (*vide infra*). The RNCE PES has much lower vibrational frequencies than the other PES, which has very similar frequencies. The underestimated frequencies lead to a lower RPMD free-energy barrier, as shown in Fig. 3, and thus larger rate coefficients.

The overall agreement of these theoretical results with experimental data is reasonably good, given the fact that the experimental results[5, 9, 14, 16-17] are quite scattered.

We note that the RPMD results on the CB PES are quite close to the experimental data of Pilgrim *et al.*[9]

The comparison for the Cl + CD_4 reaction is displayed in Fig. 4 in the same fashion as Fig. 2. Similar to the Cl + CH_4 case, the RPMD rate coefficients are slightly larger than the CUS/μOMT and CVT/μOMT counterparts on the RNCE PES, but lower on the CB PES. In the latter case, the RPMD rate coefficients are closer to the CUS/μOMT values, as expected. Also, the RPMD rate coefficients on the RNCE PES are higher than those on the CB PES. Interestingly, the latter are in better agreement with the SCTST values on a different PES.[28] The overall agreement with experimental rate coefficients,[10, 12, 15] all near 300 K, is very reasonable, given the differences among the experimental results.

The KIEs are displayed in Fig. 5 for the CH_4 and CD_4 isotopomers. The experimental values were those of Chiltz *et al.*,[4] Clyne *et al.*,[5] Wallington *et al.*,[8] Matsumi *et al.*,[10] Boone *et al.*,[12] and Feilberg *et al.*[15] For comparison, two other theoretical results, CUS/μOMT on the RNCE PES,[65] and SCTST based on *ab initio* calculations[28] are also added. It is clear from Fig. 5 that the experimental values differ considerably, even between the two newest ones. The SCTST results at 298 K are near the high end of the experimental data range, essentially following the experimental values from Clyne *et al.*[5] On the other hand, the CUS/μOMT KIEs on RNCE PES are close to the lower range of the experimental data. It is interesting that the calculated RPMD KIEs are in reasonable agreement at the two temperatures where the calculations were performed for both PESs employed in the present work, and both are in the middle of the experimental range.

IV. Conclusions

In this work, we employed recently developed full-dimensional approximate quantum mechanical method, ring-polymer molecular dynamics (RPMD), to calculate the rate coefficients and KIEs for the hydrogen/deuterium abstraction reactions of CH_4/CD_4 by the chlorine atom on two different potential energy surfaces (PESs). It is shown that these heavy-light-heavy reactions are strongly influenced by recrossing and quantum mechanical effects such as zero point energy and tunneling. Unexpected discrepancy has been found between RPMD and tunneling corrected variational transition-state theory (TST) rate coefficients at high temperatures. Depending on the underlying PES, RPMD rate coefficients can be higher or lower than the TST counterparts. In the absence of accurate quantum mechanical results for the title system, it is rather difficult to elucidate the reason for the observed discrepancy and to compare accuracy of RPMD and TST approaches. Nevertheless, the overall agreement of RPMD and TST rate coefficients with measured rate coefficients and KIEs is reasonably good, although the experimental results are quite scattered. Present results suggest that RPMD provides a reliable alternative to TST for the present system. Further investigations, including rigorous quantum mechanical calculations for the present system as well as RPMD calculations for other complex reactive systems are required for further assessing accuracy of this novel approach.

Acknowledgements: YL, HG, and WHG were supported by the Department of Energy (DE-FG02-05ER15694 to HG and DE-FG02-98ER14914 to WHG). YVS acknowledges

the support of a Combustion Energy Research Fellowship through the Combustion Energy Frontier Research Center, an Energy Frontier Research Center funded by the U.S. Department of Energy, Office of Basic Energy Sciences under Award Number DE-SC0001198. HG thanks Gabor Czakó and Joel Bowman for sending us their PES.

References:

1 A. R. Douglass, M. R. Schoeberl, R. S. Stolarski, J. W. Waters, J. M. Russell III, A. E. Roche and S. T. Massie, J. Geophys. Res.-Atmos. **100**, 13967 (1995).

2 M. L. Santee, L. Froidevaux, G. L. Manney, W. G. Read, J. W. Waters, M. P. Chipperfield, A. E. Roche, J. B. Kumer, J. L. Mergenthaler and J. M. Russell, J. Geophys. Res.-Atmos. **101**, 18835 (1996).

3 A. A. P. Pszenny, W. C. Keene, D. J. Jacob, S. Fan, J. R. Maben, M. P. Zetwo, M. Springer-Young and J. N. Galloway, Geophys. Res. Lett. **20**, 699 (1993).

4 G. Chiltz, R. Eckling, P. Goldfinger, G. Huybrechts, H. S. Johnston, L. Meyers and G. Verbeke, J. Chem. Phys. **38**, 1053 (1963).

5 M. A. A. Clyne and R. F. Walker, J. Chem. Soc. Faraday Trans. 1 **69**, 1547 (1973).

6 M. S. Zahniser, B. M. Berquist and F. Kaufman, Int. J. Chem. Kinet. **10**, 15 (1978).

7 A. R. Ravishankara and P. H. Wine, J. Chem. Phys. **72**, 25 (1980).

8 T. J. Wallington and M. D. Hurley, Chem. Phys. Lett. **189**, 437 (1992).

9 J. S. Pilgrim, A. McIlroy and C. A. Taatjes, J. Phys. Chem. A **101**, 1873 (1997).

10 Y. Matsumi, K. Izumi, V. Skorokhodov, M. Kawasaki and N. Tanaka, J. Phys. Chem. A **101**, 1216 (1997).

11 J. J. Wang and L. F. Keyser, J. Phys. Chem. A **103**, 7460 (1999).

12 G. D. Boone, F. Agyin, D. J. Robichaud, F.-M. Tao and S. A. Hewitt, J. Phys. Chem. A **105**, 1456 (2000).

13 K. Takahashi, O. Yamamoto and T. Inomata, Proc. Combust. Inst. **29**, 2447 (2002).

14 M. G. Bryukov, I. R. Slagle and V. D. Knyazev, J. Phys. Chem. A **106**, 10532 (2002).

15 K. L. Feilberg, D. W. T. Griffith, M. S. Johnson and C. J. Nielsen, Int. J. Chem. Kinet. **37**, 110 (2005).

16 R. Atkinson, D. L. Baulch, R. A. Cox, J. N. Crowley, R. F. Hampson, R. G. Hynes, M. E. Jenkin, M. J. Rossi and J. Troe, Atmos. Chem. Phys. **6**, 3625 (2006).

17 S. P. Sander, J. Abbatt, J. R. Barker, J. B. Burkholder, R. R. Friedl, D. M. Golden, R. E. Huie, C. E. Kolb, M. J. Kurylo, G. K. Moortgat, V. L. Orkin and P. H. Wine, *Chemical kinetics and photochemical data for use in atmospheric studies, Evaluation No. 17*. (JPL Publication 10-6, Pasadena, 2011).

18 M. C. McCarthy, K. A. Boering, A. L. Rice, S. C. Tyler, P. Connell and E. Atlas, J. Geophys. Res.-Atmos. **108 (D15)** (2003).

19 T. Röckmann, M. Brass, R. Borchers and A. Engel, Atmos. Chem. Phys. Discuss. **11**, 13287 (2011).

20 H. A. Michelsen and W. R. Simpson, J. Phys. Chem. A **105**, 1476 (2001).

21 K. Liu, Annu. Rev. Phys. Chem. **52**, 139 (2001).

22 S. C. Althorpe and D. C. Clary, Annu. Rev. Phys. Chem. **54**, 493 (2003).

23 C. Murray and A. J. Orr-Ewing, Int. Rev. Phys. Chem. **23**, 435 (2004).

24 D. G. Truhlar, A. D. Issacson and B. C. Garrett, in *Theory of Chemical Reaction Dynamics*, edited by M. Bear (CRC, Boca Raton, 1985), pp. 65-137.

25 W. T. Duncan and T. N. Truong, J. Chem. Phys. **103**, 9642 (1995).

26 J. Espinosa-Garcia and J. C. Corchado, J. Chem. Phys. **105**, 3517 (1996).
27 J. C. Corchado, D. G. Truhlar and J. Espinosa-García, J. Chem. Phys **112**, 9375 (2000).
28 J. R. Barker, T. L. Nguyen and J. F. Stanton, J. Phys. Chem. A **116**, 6408 (2012).
29 R. T. Skodje, Annu. Rev. Phys. Chem. **44**, 145 (1993).
30 Z. H. Kim, H. A. Bechtel and R. N. Zare, J. Am. Chem. Soc. **123**, 12714 (2001).
31 S. Yoon, R. J. Holiday and F. F. Crim, J. Phys. Chem. B **109**, 8388 (2005).
32 S. Yan, Y. T. Wu, B. Zhang, X.-F. Yue and K. Liu, Science **316**, 1723 (2007).
33 F. Wang, K. Liu and T. P. Rakitzis, Nat. Chem. **4**, 636 (2012).
34 G. Czakó and J. M. Bowman, Science **334**, 343 (2011).
35 U. Manthe, Mole. Phys. **109**, 1415 (2011).
36 G. Nyman, H. G. Yu and R. B. Walker, J. Chem. Phys. **109**, 5896 (1998).
37 H. G. Yu and G. Nyman, Phys. Chem. Chem. Phys. **1**, 1181 (1999).
38 H. G. Yu and G. Nyman, J. Chem. Phys. **110**, 7233 (1999).
39 S. Skokov and J. M. Bowman, J. Chem. Phys. **113**, 4495 (2000).
40 F. Meng, W. Yan and D. Wang, Phys. Chem. Chem. Phys. **14**, 13656 (2012).
41 Z. Zhang, Y. Zhou, D. H. Zhang, G. Czakó and J. M. Bowman, J. Phys. Chem. Lett. **3**, 3416 (2012).
42 W. H. Miller, J. Phys. Chem. **A102**, 793 (1998).
43 S. Habershon, D. E. Manolopoulos, T. E. Markland and T. F. Miller III, Annu. Rev. Phys. Chem. **64**, 387 (2013).
44 D. Chandler and P. G. Wolynes, J. Chem. Phys. **74**, 4078 (1981).
45 I. R. Craig and D. E. Manolopoulos, J. Chem. Phys. **121**, 3368 (2004).
46 I. R. Craig and D. E. Manolopoulos, J. Chem. Phys. **122**, 084106 (2005).
47 I. R. Craig and D. E. Manolopoulos, J. Chem. Phys. **123**, 034102 (2005).
48 T. J. H. Hele and S. C. Althorpe, J. Chem. Phys. **138**, 084108 (2013).
49 J. O. Richardson and S. C. Althorpe, J. Chem. Phys. **131**, 214106 (2009).
50 R. Collepardo-Guevara, Y. V. Suleimanov and D. E. Manolopoulos, J. Chem. Phys. **130**, 174713 (2009), see erratum at J. Chem. Phys. 133, 049902 (2010).
51 Y. V. Suleimanov, R. Collepardo-Guevara and D. E. Manolopoulos, J. Chem. Phys. **134**, 044131 (2011).
52 R. Pérez de Tudela, F. J. Aoiz, Y. V. Suleimanov and D. E. Manolopoulos, J. Phys. Chem. Lett. **3**, 493 (2012).
53 Y. Li, Y. V. Suleimanov, M. Yang, W. H. Green and H. Guo, J. Phys. Chem. Lett. **4**, 48 (2013).
54 Y. V. Suleimanov, R. Pérez de Tudela, P. G. Jambrina, J. F. Castillo, V. Sáez-Rábanos, D. E. Manolopoulos and F. J. Aoiz, Phys. Chem. Chem. Phys. **15**, 3655 (2013).
55 Y. Li, Y. V. Suleimanov, J. Li, W. H. Green and H. Guo, J. Chem. Phys. **138**, 094307 (2013).
56 J. W. Allen, W. H. Green, Y. Li, H. Guo and Y. V. Suleimanov, J. Chem. Phys. **138**, 221103 (2013).
57 R. Pérez de Tudela, Y. V. Suleimanov, M. Menendez, F. Castillo, and F. J. Aoiz, Phys. Chem. Chem. Phys. (2013), DOI: 10.1039/C3CP54405B..
58 J. Espinosa-Garcia, A. Fernandez-Ramos, Y. V. Suleimanov and J. C. Corchado, J. Phys. Chem. A (2014), DOI:10.1021/jp4118453.

59 C. H. Bennett, in *Algorithms for Chemical Computations, ACS Symposium Series*, edited by R. E. Christofferson (ACS, 1977), Vol. 46.
60 D. Chandler, J. Chem. Phys. **68**, 2959 (1978).
61 Y. V. Suleimanov, J. W. Allen and W. H. Green, Comput. Phys. Comm. **184**, 833 (2013).
62 R. Collepardo-Guevara, I. R. Craig and D. E. Manolopoulos, J. Chem. Phys. **128**, 144502 (2008).
63 J. Kästner and W. Thiel, J. Chem. Phys. **123**, 144104 (2005).
64 Y. V. Suleimanov, J. Phys. Chem. C **116**, 11141 (2012).
65 C. Rangel, M. Navarrete, J. C. Corchado and J. Espinosa-García, J. Chem. Phys **124**, 124306 (2006).
66 G. Czakó and J. M. Bowman, J. Chem. Phys. **136**, 044307 (2012).
67 H. C. Andersen, J. Chem. Phys. **72**, 2384 (1980).
68 J. P. Ryckaert, G. Ciccotti and H. J. Berendsen, J. Comput. Phys. **23**, 327 (1977).
69 J. C. Corchado, Y.-Y. Chuang, P. L. Fast, W.-P. Hu, Y.-P. Liu, G. C. Lynch, K. A. Nguyen, C. F. Jackels, A. Fernandez Ramos, B. A. Ellingson, B. J. Lynch, J. Zheng, V. S. Melissas, J. Villà, I. Rossi, E. L. Coitiño, J. Pu, T. V. Albu, R. Steckler, B. C. Garrett, A. D. Isaacson and D. G. Truhlar, (University of Minnesota, Minneapolis, 2007).
70 C. F. Jackels, Z. Gu and D. G. Truhlar, J. Chem. Phys. **102**, 3188 (1995).
71 Y.-Y. Chuang and D. G. Truhlar, J. Phys. Chem. A **102**, 242 (1998).
72 A. J. C. Varandas, P. J. S. B. Caridade, J. Z. H. Zhang, Q. Cui and K. L. Han, J. Chem. Phys. **125**, 064312 (2006).

Table 1. Results from RPMD calculations of the rate coefficients ($cm^3molecule^{-1}s^{-1}$) for the Cl + CH_4 reaction on the RNCE and CB PESs and comparison with other theoretical and experimental results.

T/K	300	400	600	800	1000
RNCE PES					
N_{beads}	64	32	32	16	8
$\xi^{\neq}$	0.996	0.985	0.988	0.978	0.977
$\Delta G(\xi^{\neq})$/kcal·mol^{-1}	5.40	5.74	7.98	8.09	8.58
k_{QTST}	4.02E-13	1.30E-12	5.66E-12	1.46E-11	2.87E-11
κ	0.235	0.308	0.390	0.417	0.429
k_{RPMD}	9.43E-14	4.02E-13	2.21E-12	6.06E-12	1.23E-11
CUS/μOMT[65]	9.90E-14	3.40E-13	1.60E-12	4.10E-12	8.30E-12
CVT/μOMT	1.19E-13	4.06E-13	1.81E-12	4.67E-12	9.27E-12
CB PES					
N_{beads}			32		8
$\xi^{\neq}$			0.995		0.993
$\Delta G(\xi^{\neq})$/ kcal·mol^{-1}			8.97		11.38
k_{QTST}			2.18E-12		1.31E-11
κ			0.531		0.535
k_{RPMD}			1.15E-12		7.03E-12
CUS/μOMT	4.05E-14	1.80E-13	1.09E-12	3.33E-12	7.28E-12
CVT/μOMT	6.09E-14	2.68E-13	1.64E-12	5.15E-12	1.17E-11
Expt.[9]	…	(3.0±0.2)E-13	(1.26±0.09)E-12	(3.0±0.2)E-12	…
Expt.[16]	1.00E-13	…	…	…	…
Expt.[17]	1.00E-13	3.00E-13	…	…	…

Table 2. Results from RPMD calculations of the rate coefficients ($cm^3molecule^{-1}s^{-1}$) for the Cl + CD_4 reaction on the RNCE and CB PESs and comparison with other theoretical and experimental results.

T/K	300	400	600	800	1000
RNCE PES					
N_{beads}	32	32	32	16	8
$\xi^{\neq}$	0.991	0.987	0.983	0.980	0.978
$\Delta G(\xi^{\neq})$/ kcal·mol^{-1}	6.53	7.29	8.44	9.27	9.94
k_{QTST}	2.29E-14	1.55E-13	1.45E-12	5.40E-12	1.34E-11
κ	0.483	0.520	0.557	0.557	0.569
k_{RPMD}	1.11E-14	8.06E-14	8.06E-13	3.00E-12	7.63E-12
CUS/μOMT[65]	8.84E-15	6.67E-14	6.67E-13	2.41E-12	5.53E-12
CB PES					
N_{beads}			32		8
$\xi^{\neq}$			0.995		0.993
$\Delta G(\xi^{\neq})$/ kcal·mol^{-1}			10.47		12.82
k_{QTST}			6.23E-13		6.95E-12
κ			0.645		0.607
k_{RPMD}			4.01E-13		4.22E-12
Expt.[12] (298 K)	(5.4±0.4)E-15	…	…	…	…
Expt.[8] (298 K)	(6.1±0.4)E-15	…	…	…	…
Expt.[10] (298 K)	(8.2±0.4)E-15	…	…	…	…

Figure captions:

Fig. 1. Time-dependence of transmission coefficients for the Cl + CH_4 (upper panel) and Cl + CD_4 (lower panel) reactions at different temperatures.

Fig. 2. Comparison of rate coefficients for the Cl+CH_4 reaction obtained with RPMD and TST methods on the RNCE PES (upper panel), the CB PES (middle panel) and with experimental counterparts[5, 9, 14, 16-17] (lower panel).

Fig. 3. Comparison of the potentials of mean force (PMFs) for the Cl+CH_4 reaction at 600 K obtained with RPMD on two PESs.

Fig 4. Comparison of rate coefficients for the Cl+CD_4 reaction obtained with RPMD, TST, and QCT methods on the RNCE PES (upper panel), the CB PES (middle panel) and with experimental counterparts[10, 12, 15] (lower panel).

Fig. 5. Comparison between calculated and measured KIEs[4-5, 8, 10, 12, 15] (k_H/k_D).

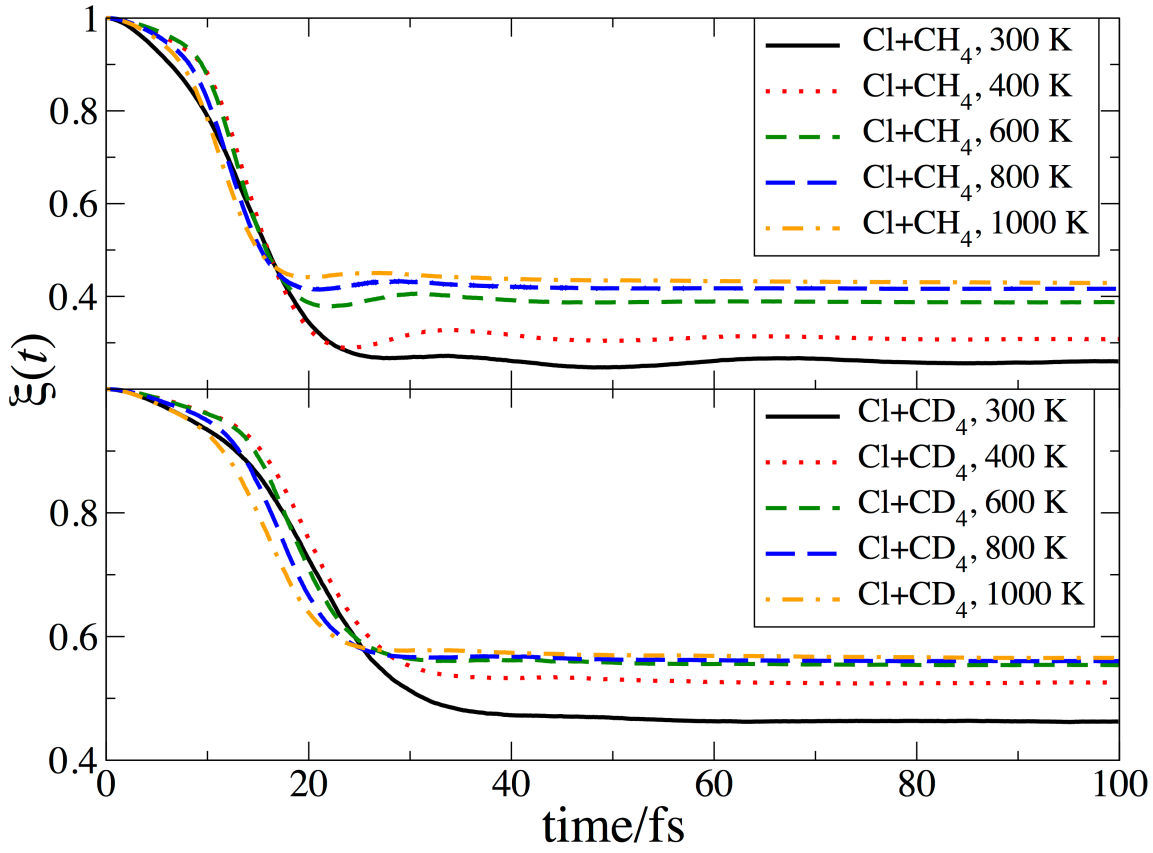
Cl+CH4, 300 K
Cl+CH4, 400 K
Cl+CH4, 600 K
Cl+CH4, 800 K
Cl+CH4, 1000 K
Cl+CD4, 300 K
Cl+CD4, 400 K
Cl+CD4, 600 K
Cl+CD4, 800 K
Cl+CD4, 1000 K
ξ(t)
time/fs
1
0.8
0.6
0.4
0
20
40
60
80
100

Fig. 1

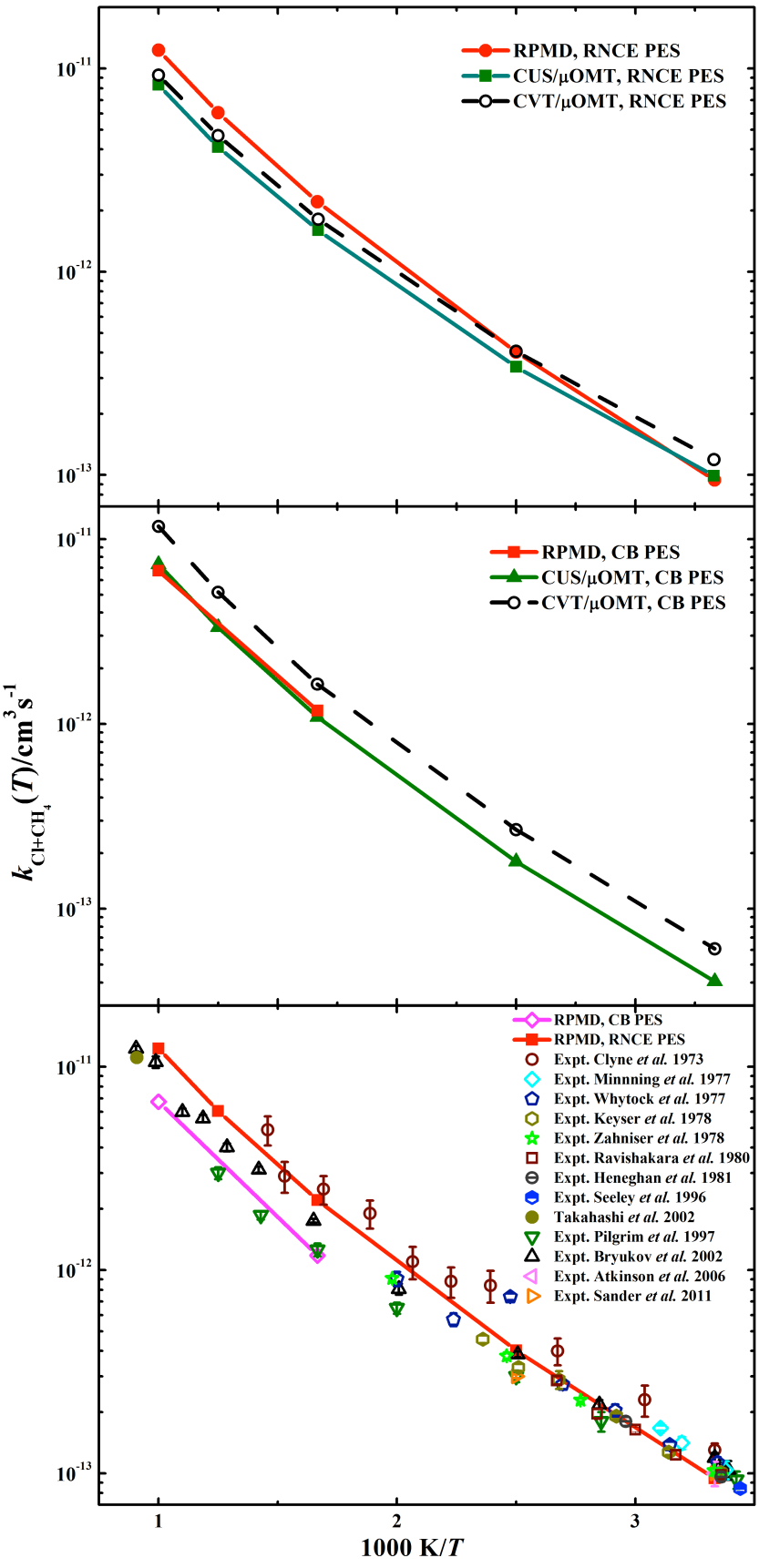
RPMD, RNCE PES
CUS/μOMT, RNCE PES
CVT/μOMT, RNCE PES
RPMD, CB PES
CUS/μOMT, CB PES
CVT/μOMT, CB PES
RPMD, CB PES
RPMD, RNCE PES
Expt. Clyne et al. 1973
Expt. Minnning et al. 1977
Expt. Whytock et al. 1977
Expt. Keyser et al. 1978
Expt. Zahniser et al. 1978
Expt. Ravishakara et al. 1980
Expt. Heneghan et al. 1981
Expt. Seeley et al. 1996
Takahashi et al. 2002
Expt. Pilgrim et al. 1997
Expt. Bryukov et al. 2002
Expt. Atkinson et al. 2006
Expt. Sander et al. 2011
$k_{Cl+CH_4}(T)/cm^3 s^{-1}$
1000 K/T

Fig. 2

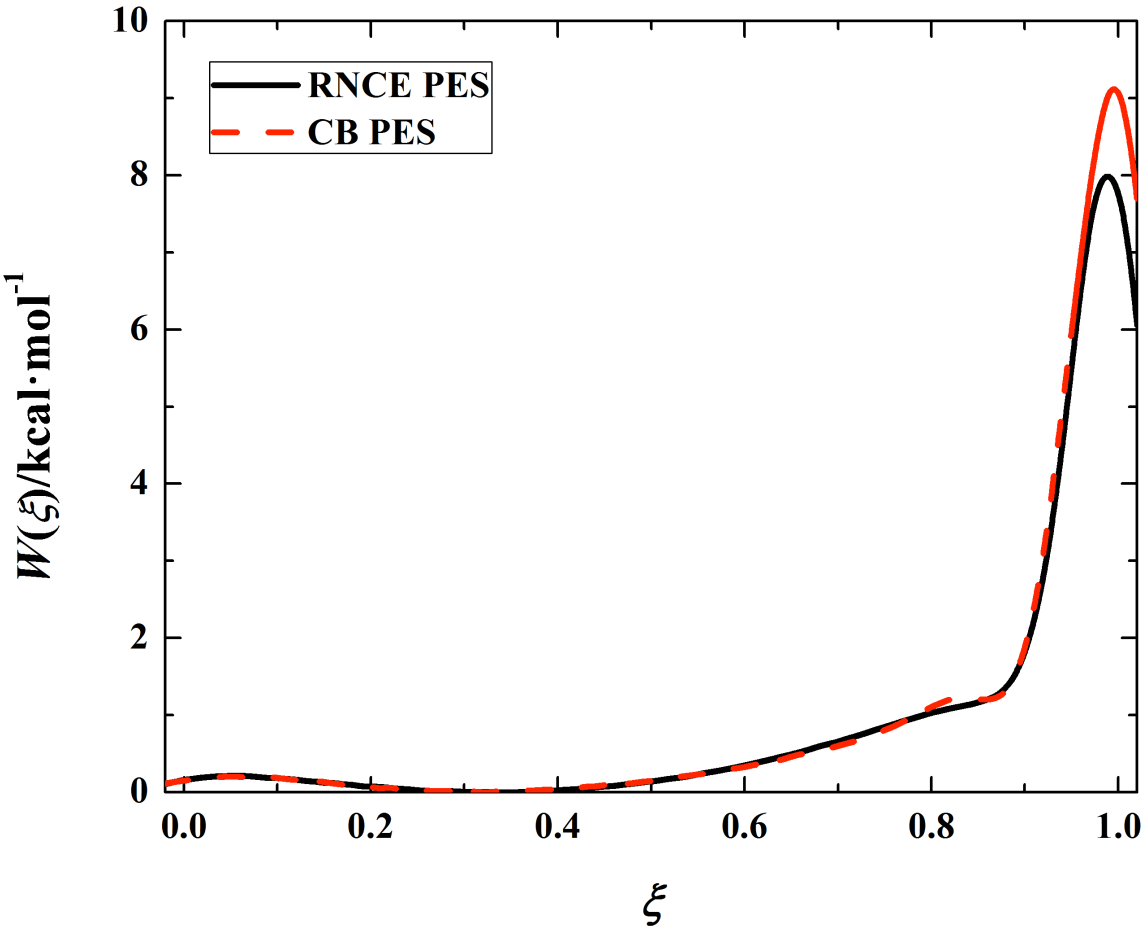

Fig. 3

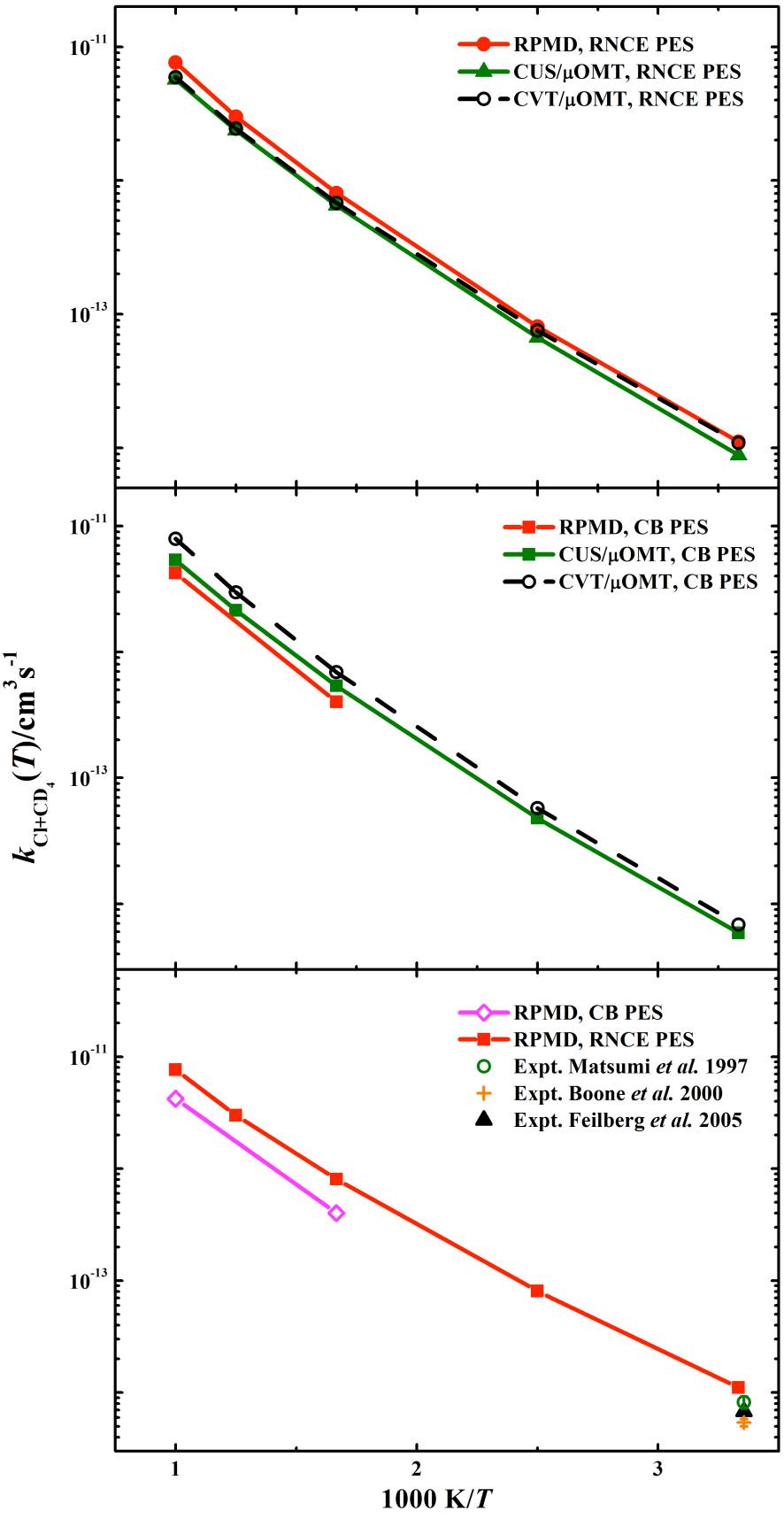
RPMD, RNCE PES
CUS/μOMT, RNCE PES
CVT/μOMT, RNCE PES
RPMD, CB PES
CUS/μOMT, CB PES
CVT/μOMT, CB PES
RPMD, CB PES
RPMD, RNCE PES
Expt. Matsumi et al. 1997
Expt. Boone et al. 2000
Expt. Feilberg et al. 2005
10^{-11}
10^{-13}
1
2
3
1000 K/T
$k_{Cl+CD_4}(T)$/cm^3 s^{-1}

Fig. 4

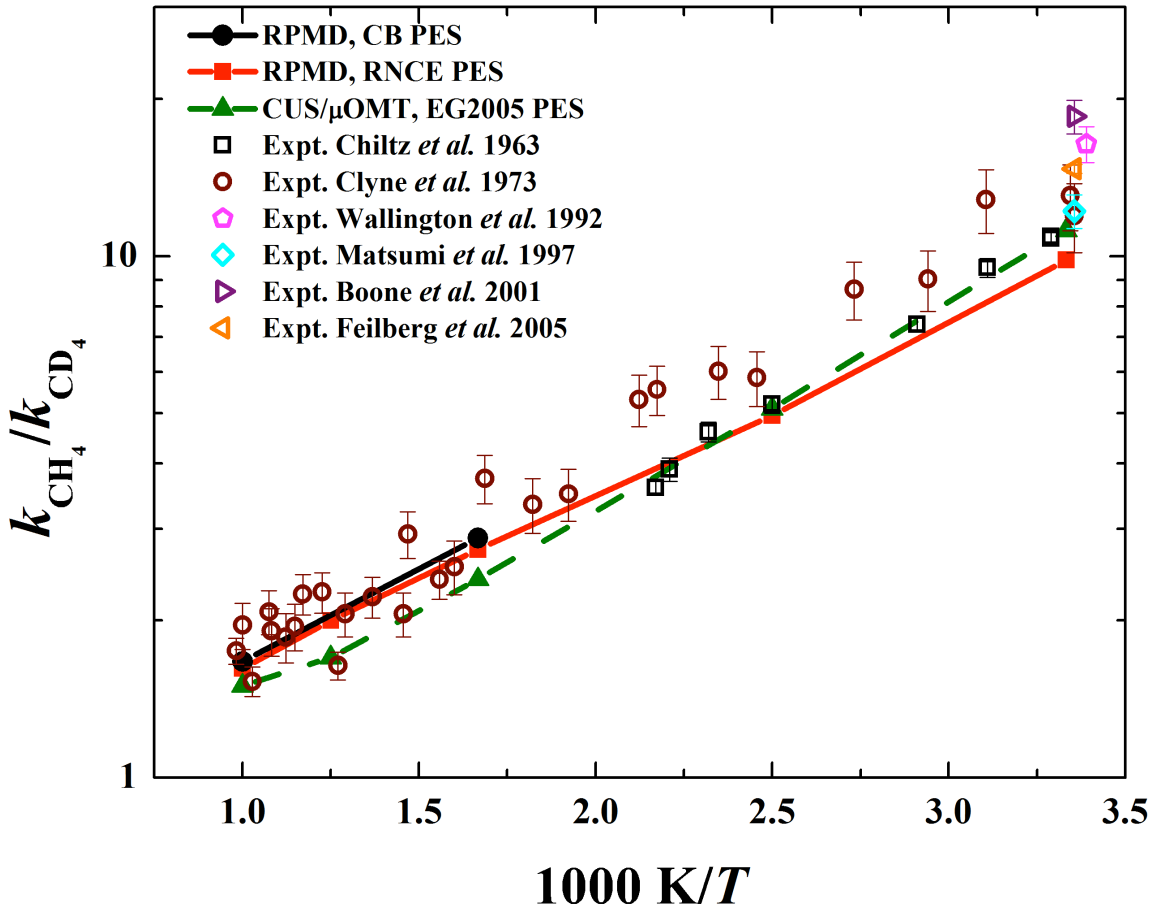
RPMD, CB PES
RPMD, RNCE PES
CUS/μOMT, EG2005 PES
Expt. Chiltz et al. 1963
Expt. Clyne et al. 1973
Expt. Wallington et al. 1992
Expt. Matsumi et al. 1997
Expt. Boone et al. 2001
Expt. Feilberg et al. 2005
10
1
1.0
1.5
2.0
2.5
3.0
3.5
1000 K/T
k_CH4/k_CD4

Fig. 5
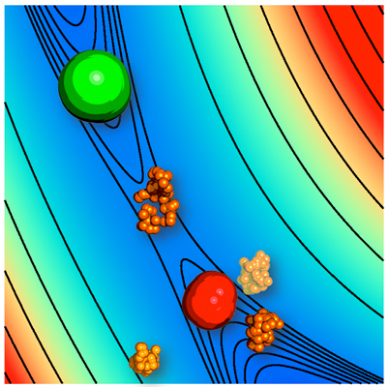
TOC graphic: